Journal of Applied Polymer Science

Incorporation of Epoxidized Soybean Oil as Co-matrix in Epoxy Resin Toward Developing Plastisol/Particulate Toughened Glass Fiber Composites

Madoor Comandore Rangasai, Subhash Hanmant Bhosale, Vismay Vinodkumar Singh, Subrata Bandhu Ghosh

Department of Mechanical Engineering, Birla Institute of Technology and Science, Pilani, Rajasthan 333031, India

Correspondence to: S. B. Ghosh (E-mail: subratabg@gmail.com)

ABSTRACT: Epoxidized soybean oil was incorporated as a co-matrix into an epoxy resin, and the hybrid resin system was used for preparing glass fiber-reinforced composites. Effect of addition of poly(vinyl chloride) plastisol and selected particulate fillers (fly ash and wood flour) to epoxy/epoxidized soybean oil matrix on mechanical and water uptake properties of glass fiber-reinforced composites were studied. Fourier transform infrared spectroscopy was used to reveal the curing state of these composites. It was observed that tensile strengths and moduli decreased with the inclusion of all additives. However, addition of poly(vinyl chloride) plastisol, fly ash, and wood flour particulate fillers showed significant increase in impact strengths compared with neat epoxy composite in a synergistic manner. Water uptake results of the composites were found to be in good agreement with —OH peak intensities obtained from Fourier transform infrared spectroscopy. Finally, acousto-ultrasonic nondestructive technique was successfully used to assess damage states and to relate stress wave factors with tensile strength properties of modified epoxy-based glass fiber composites. © 2014 Wiley Periodicals, Inc. J. Appl. Polym. Sci. **2014**, *131*, 40586.

KEYWORDS: biopolymers and renewable polymers; composites; fibers; properties and characterization; structure-property relations

Received 27 May 2013; accepted 11 February 2014

DOI: 10.1002/app.40586

INTRODUCTION

Glass fiber-reinforced thermosetting composite materials have a large number of applications by virtue of their lower density, high strength and stiffness to weight ratio, excellent corrosion resistance, dimensional stability, and low assembly costs.[1–4] The thermosetting resins are characterized by a cross-linking reaction or curing, which converts them into a three-dimensional network form. However, the main drawback associated with the application of highly cross-linked thermosetting polymers, such as epoxy resin, is related to their low toughness owing to inherent brittleness and notch sensitivity that increases with cross-link density. For load-bearing applications, this means that the product may lead to a catastrophic failure. The low toughness property also affects the mechanical durability of the epoxy composites, such as impact resistance, fatigue behavior, and damage tolerance. Enhanced toughness can be achieved through different ways: (1) reduction of the cross-linking density, (2) use of plasticizers that lead to increased plastic deformation, and (3) addition of a second phase in the form of particles. Depending on the second phase used, epoxy toughening can be grouped into four types: liquid rubber toughening, core-shell particle toughening, thermoplastic toughening and rigid particle toughening.[5] As reported by Lian et al.,[6] by increasing the toughness of the matrix, low-velocity impact resistance (desirable for structural applications) of a particulate- or fiber-reinforced composite can be improved to a greater extent. With rubber toughening, the presence of the rubber phase increases the tendency of water absorption with an accompanying loss of properties, whereas thermoplastic toughened epoxy shows higher toughness values without sacrificing much of the mechanical properties. With rigid particle toughening, incorporation of rigid fillers improve crack resistance of an epoxy resin.[7,8] In addition to performance limitations, use of thermosetting polymers for commercial applications is also sometimes limited by high cost of the product, which can be brought down by the use of low-cost easily available particulate fillers.

Currently, there is growing interest in thermosetting polymeric materials prepared from renewable natural resources owing to their biodegradability, low cost, and easy availability. Growing awareness of environmental issues, waste disposal, and the depletion of nonrenewable resources have also driven the search for alternative renewable resources based thermosetting

polymers. Plant-based natural oils are examples of such promising renewable resources. Soybean oil, for example, is an inexpensive, readily available, renewable natural oil with multiple sites of reactivity, including ester and olefinic sites, which provide an excellent platform for functionalization. As a biodegradable and renewable raw material, functionalized soybean oil is widely used for the modification (e.g., as plasticizers or stabilizers) and preparation of different polymers (mostly polyesters and polyurethanes).

Composites Containing Natural Oil Resin

Functionalized natural oils such as epoxidized soybean oil (ESBO) have been at the research focus to replace or augment the traditional petroleum-based polymers and resin.[9] Although abundant and inexpensive, ESBO alone as a material does not offer satisfactory mechanical performance properties, such as strength and rigidity, which limits their use in the marketplace. A common approach is to use ESBO as co-matrix to make blends/composites of ESBO and other synthetic resins to produce materials of competitive performance and a low overall cost with improved processability.[10,11] Generally, epoxy resins offer very good miscibility with ESBO, and the typical hardener used for epoxy resin can also be used for the resin blend.[11] Liu et al.[12] prepared soybean oil-based composites by the solid free forming fabrication method, and composites were formed by glass and carbon fiber reinforcements. Karger-Kocsis et al.[13] studied the effects of incorporation of ESBO in a standard bisphenol A-type epoxy resin cured by anhydride hardener. Wang and Schuman[14] reported the use of glycidyl esters of epoxidized fatty acids derived from soybean oil. The results showed that the dilution of epoxy resin (diglycidyl ether of bisphenol A [DGEBA]) with ESBO was accompanied with marked changes in the curing behavior, intermolecular cross-linking, and glass-transition temperature. The use of ESBO in epoxy resin and the resultant mechanical properties have also been studied by Zhu et al.[15] and Parzuchowski et al.[16] Chlorinated soy epoxy resin has also been used as a co-resin with glass fiber reinforcements using *m*-phenylene diamine as the curing agent.[17] The study investigated the mechanical properties such as tensile strength (248–299 MPa) and tensile modulus (2.4–3.4 GPa) of the fabricated composites and concluded that the incorporation of up to 15%–20% of soy-based epoxy resin led to a decrease in mechanical and thermal properties. However, all these studies reported that although the epoxidized vegetable oils based thermosetting materials are promising, they tend to suffer from shortcomings in terms of poor mechanical properties and high degree of water uptake. The hydroxyl groups in ESBO tend to attract water molecules, as they are polar in nature. The water molecules absorbed in ESBO may exist as bound water or unbounded cluster.

Acousto-Ultrasonic Nondestructive Technique

One major challenge in the bioresource-based composite technology is the use of an appropriate method to understand the fiber breakage during compounding and its effect on mechanical performance. Acousto-ultrasonic (AU) inspection technique is of special interest in this respect. AU technique uses stochastic wave propagation to detect and quantify defect states, damage conditions, and variations in mechanical properties in fiber-reinforced composites. AU technique is more concerned with characterization of damage state of the composite material through evaluation of the integrated effect of diffuse populations of subcritical flaws than with overt flaw detection. It is known that damages or defects like porosity, matrix crazing, fiber bunching, fiber breaks, resin richness, poor curing, and poor fiber–matrix bonding also influence AU measurements.[18,19] Another important aspect of the AU study is to quantify AU signals with variations in mechanical properties like tensile strength.[20] The measurements are made by means of a stress wave factor (SWF). The SWF is described as a measure of the efficiency of stress wave energy transmission.

Against this background, our work was aimed to use ESBO as a co-matrix in the presence of two different categories of fillers (organic and inorganic) and thermoplastic poly(vinyl chloride) (PVC) polymer-based plastisol (a suspension of fine particles of PVC). We report the effect of incorporation of ESBO along with PVC plastisol, wood flour, and fly ash on the mechanical behavior and water uptake of glass fiber epoxy composite laminates. We expect that modified ESBO/DGEBA blend will yield materials that are stronger than materials obtained from commercially available unmodified ESBO. It is hypothesized that the use of PVC plastisol/filler combination will enhance the toughness and thereby the impact strength properties of the composite. We also expect that the plasticization effect of ESBO will reduce the inherent brittleness of epoxy resin which in turn will further enhance the impact toughness of composite laminates in a synergistic manner. The effects of selected fillers on mechanical and water uptake properties are discussed. Damage assessment of composites was carried out by AU technique, and the results were correlated with ultimate tensile strengths of the composites.

EXPERIMENTAL

Materials

DGEBA with a density of 1.6 g cm^{-3} was used as the synthetic epoxy resin. Triethylenetetramine (TETA) was used as the curing agent. Chopped E-glass nonwoven mat was purchased from Saint Gobain, India, having areal density of 479 g m^{-2} and 40% glass fiber content (manufacturer data). Commercial ESBO with density of 0.92 g cm^{-3} was used. Commercial PVC plastisol was used with 50% resin volume fraction. The epoxide equivalent weight (EEW) of DGEBA was 185 and that of ESBO was calculated to be 206. The average particle size of wood flour was 150 μm and that of fly ash was 100 μm. All chemicals were procured from Kay Bee Polymers, Gurgaon, India.

Composite Fabrication

Different resin blend compositions (DGEBA/ESBO) for preparing the glass fiber epoxy composites are listed in Table I. DGEBA and ESBO in specific proportions (Table I) were heated and mixed well at a temperature of 70°C for 1 hour in a magnetic stirrer (RCT basic IKAMAG), which ensured reduced viscosity and homogeneous mixing of resin blend. ESBO content was kept low, as increase in ESBO might lead to phase separation, owing to lower cross-linking density of ESBO compared with synthetic DGEBA which in turn would lead to poor

Table I. Compositions of Different Types of Glass Composites (in Parts Per Hundred Resin (phr) Based on 100 Parts of DGEBA)

Sample number	DGEBA	ESBO	PVC plastisol	Fly ash	Wood flour
1	100	-	-	-	-
2	100	25	-	-	-
3	100	25	5	-	-
4	100	20	-	30	-
5	100	20	-	-	20

mechanical strength.[17] The resin blends were found to be transparent, indicating that the resin blends were not phase separated. These findings are consistent with those of Miyagawa et al.[10,21] and other researchers[4] who observed that at only above 30 wt % of ESBO in synthetic epoxy resin the blend became nontransparent, indicating possible phase separation.

To investigate the effect of incorporation of PVC plastisol, 5 parts per hundred resin (phr) PVC plastisol was added in a blend consisting of 25 phr ESBO. The mixture was then degassed under vacuum to remove entrapped air bubble before adding TETA (curing agent). TETA (15% by weight of DGEBA) was then added at 70°C and stirred for 5 min. The percentage of TETA added to the mixture for hardening was kept at a constant 15% for all compositions (stoichiometric 11.5%). The hardener percentage of 15% was found to be appropriate to ensure complete reaction, as higher amounts (>15%) resulted in too brittle composites. Composite containing neat DGEBA only was also prepared as a control for comparison. Because addition of plasticizer and fillers affect resin curing,[22] ESBO and filler contents were adjusted to ensure proper curing of the glass fiber-reinforced composite laminates. Thus, 30 phr fly ash and 20 phr wood flour were incorporated into glass fiber composites, with the matrix blend consisting of 20 phr ESBO. Wood flour was dried at 110°C for 2 hours in an oven before adding to the mixture. Composite samples of size 17 cm × 15 cm were prepared using the hand lay-up technique, which were then allowed to cure at room temperature for 24 hours. The cured samples were found to be transparent, indicating nonseparation of the epoxy/ESBO mixture. Specimens were then cut into the specified dimensions for mechanical testing.

Fourier Transform Infrared Spectroscopy

Samples were analyzed by Fourier transform infrared spectroscopy (FT-IR) using a Shimadzu IRPrestige-21 Spectrophotometer to study the state of curing. Samples were studied in the 400–4000 cm^{-1} range for 16 scans. Potassium bromide powder was used while scanning the reference spectrum, and all the varying combinations were scanned with a mixture of finely ground potassium bromide powder and the samples.

Water Absorption Tests

Three samples for each formulation were cut into dimensions of 50 mm × 15 mm × 4 mm and dried in an oven at 110°C for 2 hours. The dried samples were then weighed and immersed in static distilled water bath maintained at a temperature of 25°C and 25% relative humidity, with a water surface level 50 mm above the top surface of specimens. Water uptake values of the samples were measured after every 24 hours by removing them from water bath and wiping until the values showed saturation in water absorption of the specimens.

Tensile Tests

Specimens for tensile tests were carefully cut into sizes of 170 mm × 15 mm × 4 mm. Tensile strength testing of rectangular specimens of 100 mm gauge length was performed on a Unitek 94100 Electronic Universal Testing Machine (FIE, India) with a constant cross head speed of 5 mm min^{-1} as per ASTM D638-03 standard. Load was measured using a load cell of 100 kN capacity. Five samples of each type were tested to account for possible variations in results.

Impact Tests

The impact energy absorption was measured by performing unnotched Charpy impact tests on glass fiber-reinforced composites of different matrix compositions. In this investigation, an impact testing machine (FIE, India), with the pendulum hammer having a mass of 20 kg and a swing arm length of 820 mm leading to a speed at impact of around 5 m s^{-1} and a stored energy of 300 J, was used. The specimen dimensions were 55 mm × 10 mm. Samples were held in simply supported manner with a support span length of 40 mm.

Acousto-Ultrasonic Tests

The instrument used for AU nondestructive testing was Portable Pocket AU System (Physical Acoustic Corp., Princeton Jct, NJ, USA). The instrument consisted of a pocket personal computer and an AU board with rolling sensor probes. Using a broad band transducer of 250 kHz frequency, ultrasonic pulses were injected by the pulser into the materials. Rolling sensor probes were covered with silicon rubber pads, which acted as dry couplant. The specimen surface was cleaned before starting the scanning. The probe pocket was pressed firmly against the specimen to avoid changes in pressure during the time the pulser was activated. This reduced the chance of erroneous acoustic signals emanating from the fixture itself or from friction noises caused by the sensor sliding over the specimen. These experiments were performed at a time of minimum noise interference. The amplitude of the captured AU signal was extracted and plotted on the corresponding position along the scanning line by the AU software. The ultimate purpose of the AU approach is to rate the relative efficiency of stress wave propagation in a material. For many materials, better stress-waves energy transfer means better transmission of dynamic strain and better load distribution. Accordingly, the working hypothesis is that more efficient stress (or strain) energy flow and distribution corresponds to increased strength and fracture resistance in composites. This hypothesis is based on the "stress wave interaction" concept, which holds that spontaneous stress waves at the onset of fracture promote rapid catastrophic cracking unless their energies are dissipated or absorbed. Prompt and efficient flow of stress wave energy away from crack nucleation sites is desired when the energy cannot be absorbed locally without crack formation. It is for the purpose of precisely gauging the relative efficiency or impedance of stress wave energy flow that the AU approach was conceived. After the inspection was finished, the

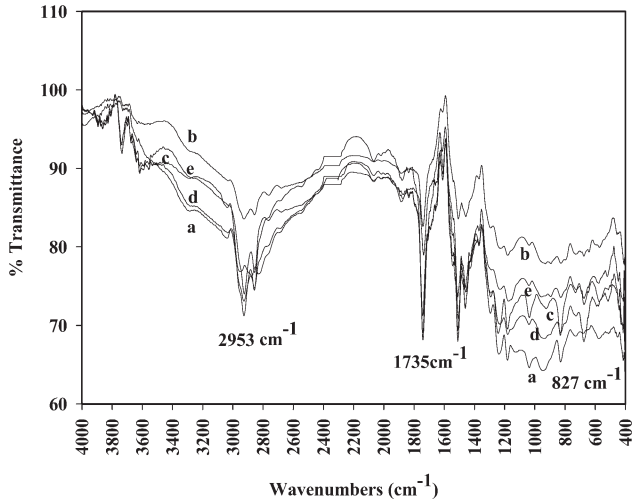

Figure 1. FT-IR spectra of glass fiber-reinforced composites with matrix containing (a) neat DGEBA, (b) DGEBA/ESBO, (c) DGEBA/ESBO + PVC plastisol, (d) DGEBA/ESBO + fly ash, and (e) DGEBA/ESBO + wood flour.

C-scan data file was stored in the flash memory of the system and retrieved later for analysis. The files were exported in ASCII format and were analyzed for peak amplitudes using Microsoft Excel.

RESULTS AND DISCUSSION

Fourier Transform Infrared Spectroscopy

Figure 1(a) shows the FT-IR spectra of the prepared composite specimens. The peak at 3037 cm^{-1} corresponds to the —CH stretching of the terminal oxirane ring in DGEBA. The peak at 2875 cm^{-1} is attributed to the aliphatic —CH stretching whereas the peak at 2953 cm^{-1} arises due to the —CH stretch of the aromatic phenyl ring. The presence of a peak at 1735 cm^{-1} can be attributed to the ester groups that are present in ESBO. At 1608 cm^{-1}, a peak is observed as a result of the C=C stretching of the aromatic ring. Similarly, 1508 cm^{-1} shows a peak for the C—C stretching of the phenyl ring. The peak at 1180 cm^{-1} is an indication of the Si—O—Si (siloxane) bond in glass fiber. Peaks are also observed at 945 and 829 cm^{-1}, which can be ascribed to the C—O and C—O—C stretching vibrations of the oxirane group, respectively. The peak at 768 cm^{-1} is from the rocking of the CH_2 group in the oxirane ring.

In Figure 1(b–e), the spectrum shows the presence of an epoxy group at 827 cm^{-1}. However, Lakshmi and Reddy,[23] reported the disappearance of the epoxy group peak due to stretching at 830 cm^{-1} as a result of reaction with the amine group. This can be clearly explained as due to the presence of ESBO, which is a part of the cured matrix. The addition of fly ash as a filler along with ESBO lead to the emergence of new peak in Figure 1(d) at 1051 cm^{-1}, which can be ascribed to Si—O stretching vibrations. The replacement of fly ash by wood fiber as a filler in sample [Figure 1(e)] showed a broad band of spectrum from 3500 to 3000 cm^{-1} that is attributed to the intermolecular —OH stretching. The broader spectrum compared with the —OH spectrum of fly ash can be attributed to a larger number of —OH groups that is present in the glucose units of the wood cellulose polymers.[24,25]

FT-IR results also revealed the absence of overlapping amine groups in the —OH stretching region (3000–3500 cm^{-1}), which indicated the nonavailability of reactive amine groups (primary and secondary amines), which in turn indicated the cured state of the composites. The presence of fly ash further decreased the intensity of the hydroxyl group because of its hydrophobic nature, whereas addition of wood flour led to an increase in the intensity of the —OH band owing to its hydrophilic nature.

Water Absorption Tests

The water uptake capacities of different glass fiber composites are shown in Figure 2. Water uptake of these samples at time t is calculated using eq. (1).

$$\%\,\text{Water uptake} = \frac{M_t - M_0}{M_0} \times 100 \quad (1)$$

where M_t is the mass of sample exposed to water absorption at time t and M_0 is the mass of dry sample at the start of the water absorption test. Glass fiber composite with neat DGEBA showed water uptake capacity of 6.6%, and the sample with 25 phr ESBO showed a capacity of 12.1%. Figure 2 shows that water uptake of all composites reach the saturation stage at approximately 12 days, indicating that the water uptake of all composites have achieved the equilibrium condition, in which stage, all the microvoids in the three-dimensional cross-linked network structure are filled with water molecules.[26] Besides, the incorporation of ESBO into the cross-linked structure of epoxy resin resulted in reduction of cross-linking density.[27] Consequently, an increase in water uptake was observed as ESBO was introduced into DGEBA matrix, and this can be attributed to the presence of polar groups in ESBO, the difference in free volume,[28] and reduced cross-linking density.[27] On the other hand, composites with 25 phr ESBO and 5 phr PVC plastisol showed a reduced water uptake of 6.7%. This water uptake capacity is

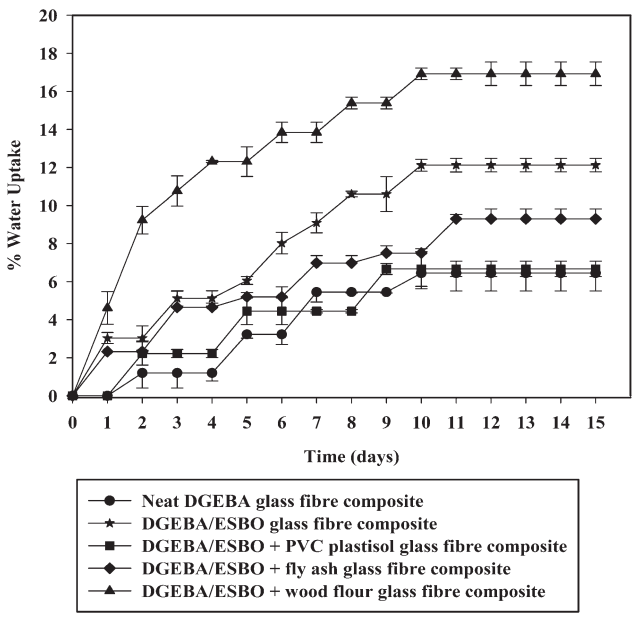

Figure 2. Water uptake values of various glass fiber composites.

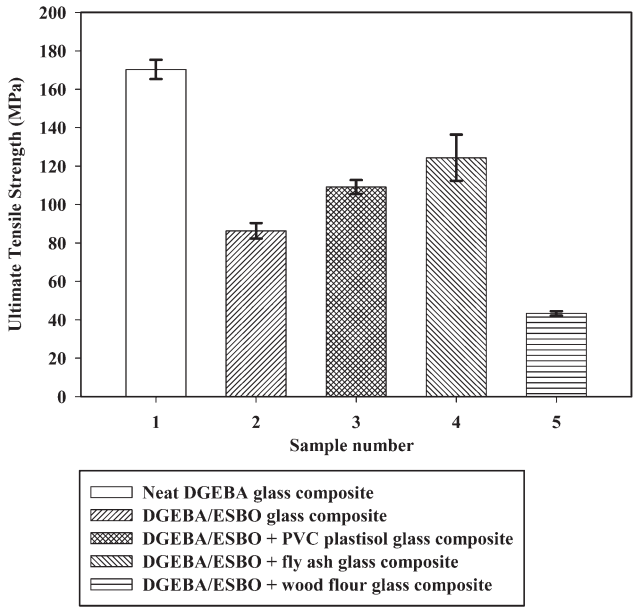

Figure 3. Ultimate tensile strengths of different types of glass fiber composites.

comparable with composites with neat DGEBA. This can be attributed to good intermolecular adhesion properties of hydrophobic PVC plastisol (fine dispersion of PVC particles) in the matrix, making it more compact. The addition of wood flour and fly ash particulates to the glass fiber composites with ESBO yielded varying results. The addition of wood fiber markedly increased the water uptake content to 16.9% compared with 12.1% without filler, whereas the addition of fly ash reduced this to 9.3%. The former result can be attributed to the highly hydrophilic nature of wood fiber, whereas the latter can be ascribed to the hydrophobic nature of fly ash. The water uptake results were in good agreement with the trend observed in —OH peak intensities from FT-IR results: composites with higher —OH peak intensities registered higher water uptake values. The variation in moisture absorption among the different samples of the same formulation, indicated by error bars in Figure 2, might be due to the microcracks introduced into the samples during the machining of the samples.[29]

Tensile Tests

Ultimate tensile strengths and tensile moduli of different glass fiber epoxy composites are shown in Figures 3 and 4, respectively. Ultimate tensile strength and tensile modulus for neat DGEBA-based glass fiber-reinforced composite were found to be 170 and 2548 MPa, respectively. It was observed that with the addition of 25 phr ESBO in the matrix, both ultimate tensile strength and the tensile modulus of samples decreased to 86 and 1638 MPa, respectively. A decreasing trend in tensile strength and modulus of composites with addition of ESBO in DGEBA can be interpreted in terms of plasticization effect—the addition of soft segments of ESBO into the epoxy resins reducing the rigidity of the epoxy network, thus resulting in decrease in the tensile strength modulus of glass fiber composite.[30] Another reason could emanate from the structure of ESBO, which contains less cross-linking sites between the chains having less epoxy groups compared with DGEBA. This allows more slipping of the chains, thereby increasing the ductility.[22] Similar trends with decreasing tensile strength and modulus values were also reported by other researchers.[9,15,17,22,27,31,32] However, it was interesting to note that addition of 5 phr PVC plastisol to the matrix consisting of 25 phr ESBO resulted in an increase in both ultimate tensile strength and tensile modulus to 109 and 1835 MPa, respectively. This could be well attributed to the improved interfacial adhesion between fiber and matrix and better blend compatibility with incorporation of hydrophobic PVC plastisol. When 30 phr fly ash was added to the matrix containing ESBO, the tensile strength and moduli values were found to be 124 and 2243 MPa, respectively. With incorporation of wood flour to the ESBO/DGEBA matrix of the glass fiber composite, ultimate tensile strength and tensile modulus of the samples were found to be 43 and 488.5 MPa, respectively, which was significantly less when compared with glass fiber-reinforced composite consisting of neat DGEBA matrix, as was observed also by previous researchers.[33] Formation of agglomerates due to strong polarity of hydroxyl groups of wood flour, possibly led to increased filler–filler interaction (through hydrogen bonds), thereby resulting in increased number of defect sites and poor interfacial interactions. This in turn, could lead to inefficient stress transfer within the composite and could be attributed to the decrease in mechanical properties of particulate filled composite.[25] Decrease in strength could also stem from the inability of the irregularly shaped wood flour to withstand stresses transferred from the matrix. Zaini et al.[34] studied the effect of wood flour on the mechanical properties of polypropylene/oil palm composites, which showed a similar trend. Another reason for lower strength could be attributed to the presence of high lignin content in wood flour. It was observed in an earlier study by Klason et al.[33] that lignin influences the adhesion between fibers and matrix.

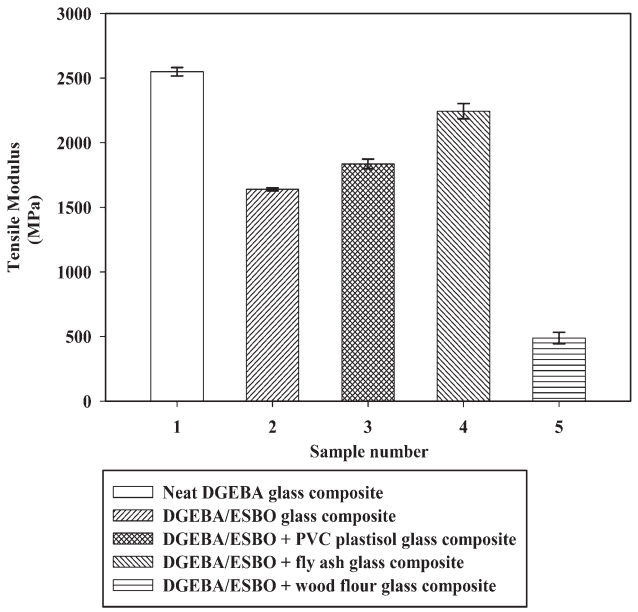

Figure 4. Tensile moduli of glass fiber composites.

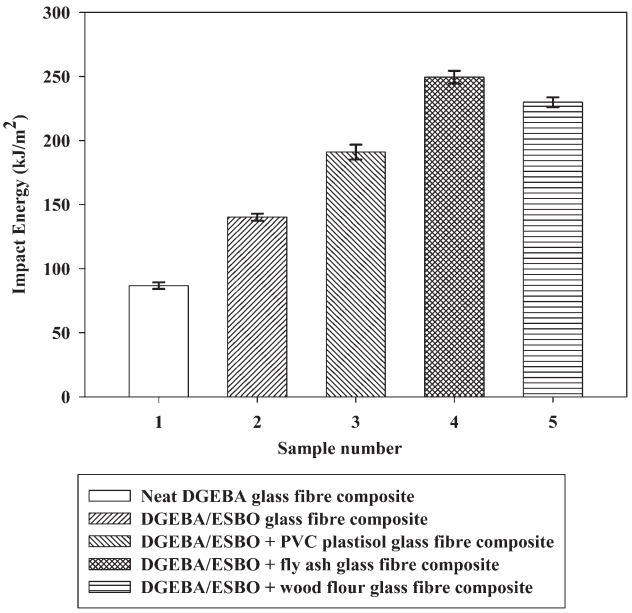

Figure 5. Impact strengths for various glass fiber composites.

Impact Tests

Figure 5 shows the Charpy impact test results of glass fiber-reinforced composites prepared with different matrix compositions. Impact strength was expressed in terms of energy absorbed per unit cross-sectional area (J m^{-2}). The purpose of carrying out impact test was to determine the effect of addition of ESBO, PVC plastisol, and fillers on impact toughness of the glass fiber-reinforced composites. Impact strength for glass fiber-reinforced composite with neat DGEBA was found to be 89.4 kJ m^{-2}. Glass fiber composites prepared with addition of 25 phr ESBO to DEGBA matrix registered a value of 140.4 kJ m^{-2}, showing an increase of around 57% in impact strength over neat DGEBA glass fiber composite. This could be attributed to the introduction of the flexible aliphatic chain of ESBO into the epoxy matrix, which led to a decrease in the internal stress of the network.[17–20] Furthermore, reduced cross-linking density or toughening agent in ESBO moieties, acting as a plasticizer in the blends, could also be responsible for improved impact strength properties of ESBO-modified resin composites.[32,35]

Addition of 5% PVC plastisol to the blend consisting of 25 phr ESBO further increased the impact strength to 193 kJ m^{-2}. This increase may be attributed to "thermoplastic toughening" effect where molecules of PVC plastisol in the DGEBA/ESBO blend act as "soft points," absorbing the impact and thus changing the mechanism of fracture.[36] A further and significant improvement in impact strength was observed when 30 phr fly ash was added to the synthetic epoxy resin matrix containing 20 phr ESBO. Impact strength was increased by 184% compared with glass fiber-reinforced composite with neat DGEBA, registering a value of 254.5 kJ m^{-2}. Such an increase in impact strength could be attributed to the fine particle sizes of fly ash with large surface area, leading to an increase in impact energy absorption of the glass fiber-reinforced composite. Also, the presence of fly ash particle could be responsible for resisting crack growth movement, as growing crack front has to change numerous paths and hence higher energy absorption before fracture.[3] Impact energy of glass fiber-reinforced composite with 20 phr wood flour also registered a high value of 228 kJ m^{-2}, which was 150% more

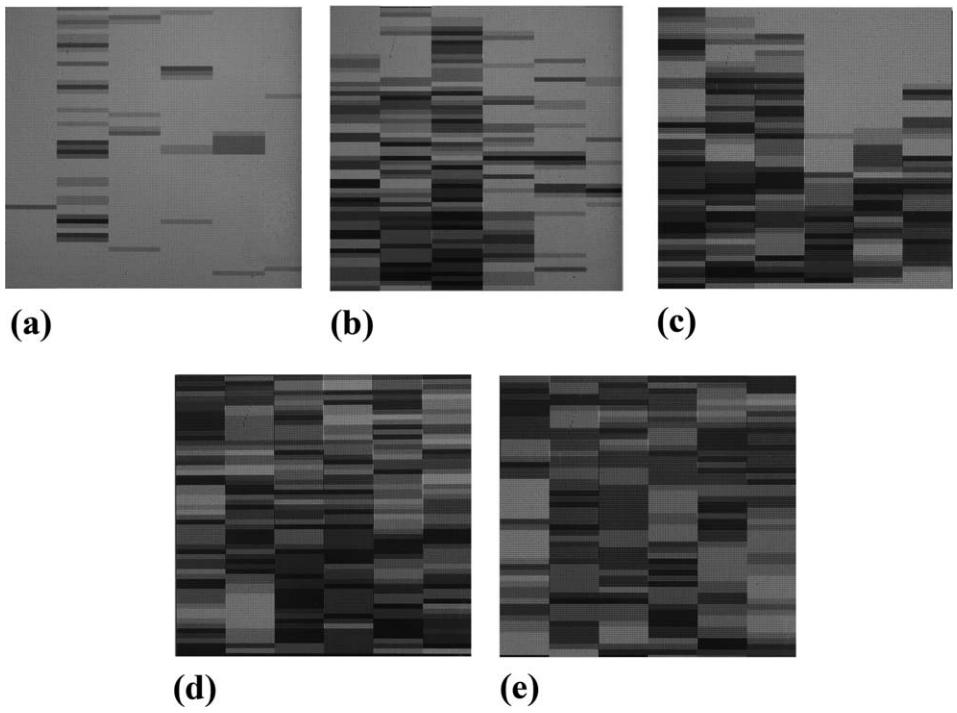

Figure 6. Acousto-ultrasonic C-scan images of glass fiber-reinforced composites with matrix containing (a) neat DGEBA, (b) DGEBA/ESBO + fly ash, (c) DGEBA/ESBO + PVC plastisol, (d) DGEBA/ESBO, and (e) DGEBA/ESBO + wood flour.

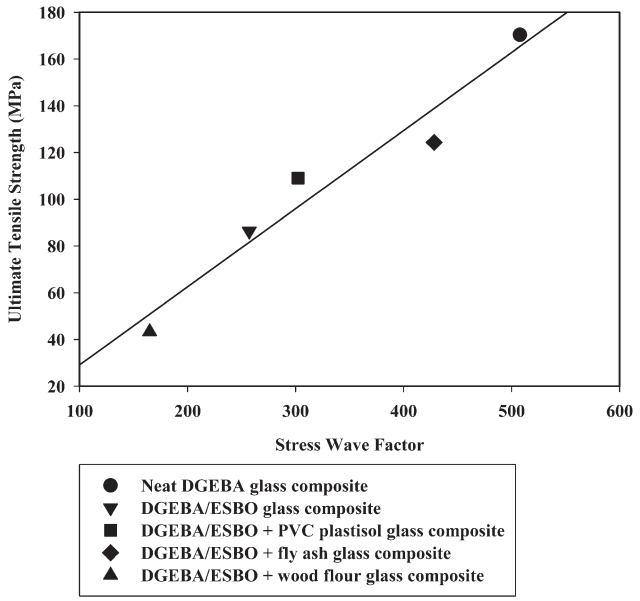

Figure 7. Ultimate tensile strength versus stress wave factor for different types of glass fiber composites.

than that of neat DGEBA glass fiber-reinforced composite. Presence of wood flour in the matrix might have provided good resistance to the fracture paths, owing to shear yielding and crack pinning, leading to an increase in impact strength. The variations in impact strength among samples of the same composition might be due to the possible variation in impregnation of the glass fibers with epoxy/ESBO blend because of the hand lay-up process.

Acousto-Ultrasonic Tests

Figure 6 shows C-scans of different glass fiber-reinforced composites. C-scans are qualitative representation of the composite in terms of defects, flaws, and weak interfacial bonds. Darker areas in the images represent flaws in the specimen. Figure 6 shows the overall damage stage states of the composites, with increasing damages revealed as we move from Figure 6a to 6e. The qualitative information obtained from C-scan images was then investigated to correlate with ultimate tensile strengths of different composites. The quantitative correlation was made through the determination of SWF values using peak amplitudes obtained from AU measurements. Lower values of SWF generally correspond to regions of higher attenuation. One of the methods of defining SWF is as follows:

$$\mathrm{SWF} = V_{\max} \tag{2}$$

where $V_{\max}$ = maximum (peak-to-peak) voltage oscillation. This SWF formulation assumes that the peak amplitude varies with the defect state of the material being examined. Figure 7 shows variation of ultimate tensile strengths of the composites against corresponding values of the SWF. The results indicate that SWF increases with increasing ultimate tensile strength of glass fiber-reinforced composites and that peak amplitude method of determining SWF could be succesfully used to assess composite mechanical properties. The qualitative assessment from AU measurement data, therefore, was supported by quantitative tensile strength data.

CONCLUSIONS

Glass fiber-reinforced composites with a modified matrix of epoxy resin based on DGEBA and ESBO were prepared. To investigate the effect of addition of PVC plastisol and fillers to DGEBA/ESBO matrix, different glass fiber specimens were prepared. FT-IR studies revealed the absence of any amine group peak, which indicated the cured state of the composites. Also, reduced hydroxyl group (—OH) stretching intensities were observed for composites having plastisol and fly ash, whereas samples with only DGEBA/ESBO and wood flour displayed higher —OH stretching intensities. The observations were in good agreement with the water absorption test results. Water absorption tests indicated an increase in water uptake with addition of ESBO to DGEBA matrix. The use of PVC plastisol in DGEBA/ESBO matrix led to a decrease in water absorption compared with the DGEBA/ESBO matrix composite. Composites with particulates showed a varying trend, with specimen having fly ash showing less water uptake, which could be attributed to the hydrophobic nature of fly ash, whereas use of wood flour showed an increase in water uptake because wood flour is hydrophilic by nature. The tensile moduli and tensile strengths of glass fiber-reinforced composites decreased with introduction of ESBO into the DGEBA matrix. This could be attributed to reduction in cross-linking density as a result of presence of ESBO in the matrix. Addition of fly ash resulted in a decrease in tensile modulus and tensile strength values compared with neat DGEBA, whereas use of wood flour showed very low values, which may be ascribed to poor interfacial compatibility, formation of agglomerates, and presence of lignin in wood flour. Impact test results showed a reverse trend when compared with tensile test results, as addition of ESBO led to an increase in impact strength compared with neat DGEBA, which could stem from the introduction of soft segments from larger-molecular-weight ESBO into the epoxy resins. Incorporation of PVC plastisol, fly ash, and wood flour to DGEBA/ESBO matrix further increased the impact strength of glass fiber-reinforced composites in a synergistic manner, owing to the possible plasticization effect of ESBO, "thermoplastic toughening" of PVC plastisol, and "particulate toughening" effects from particulates. Nondestructive evaluations of all specimens were done using AU technique to have a qualitative damage assessment of the glass fiber-reinforced composites. C-scan images of the specimens obtained after AU scanning depicted qualitatively the integrated state of defects, which ultimately represented the mechanical properties of those specimens. Specimens with larger defect regions displayed lower tensile strengths. To quantitatively analyze the AU scans, peak amplitude method of SWF was used, and the results indicated that peak amplitude method could be succesfully used to assess tensile strength propeties of the composites.

REFERENCES

1. Hull, D.; Clyne, T. W. An Introduction to Composite Materials; Cambridge University Press: Cambridge, UK, **1996**.
2. Khot, S. N.; Lascala, J. J.; Can, E.; Morye, S. S.; Williams, G. I.; Palmese, G. R.; Kusefoglu, S. H.; Wool, R. P. *J. Appl. Polym. Sci.* **2001**, *82*, 703.

3. Gupta, N.; Brar, B. S.; Woldesenbet, E. *Bull. Mater. Sci.* **2001**, *24*, 219.
4. Rahman, M. M.; Zainuddin, S.; Hosur, M. V.; Robertson, C. J.; Kumar, A.; Trovillion, J.; Jeelani, S. *Compos. Struct.* **2013**, *95*, 213.
5. Ratna, D. In Rapra Review Reports; Gardiner, M. F., Ed.; Rapra Technology: Shrewsbury, UK, **2005**, 9.
6. Lian, J. Y.; Jang, B. Z.; Hwang, L. R.; Wilcox, R. C. *Plast. Eng.* **1988**, *44*, 33.
7. Amdouni, N.; Sautereau, H.; Gerard, J. F. *J. Appl. Polym. Sci.* **1992**, *46*, 1723.
8. Amdouni, N.; Sautereau, H.; Gerard, J. F.; Fernagut, F.; Coulon, G.; Lefebvre, J. M. *J. Mater. Sci.* **1990**, *25*, 1435.
9. Vaidya, R.; Chaudhary, G.; Raut, N.; Shinde, G.; Deshmukh, N. International Conference on Environmental, *Biomedical and Biotechnology IPCBEE*; **2012**, *55*, IACSIT Press, Singapore.
10. Miyagawa, H.; Mohanty, A. K.; Misra, M.; Drzal, L. T. *Macromol. Mater. Eng.* **2004**, *289*, 636.
11. Gupta, A. P.; Ahmad, S.; Dev, A. *Polym. Eng. Sci.* **2011**, *51*, 1087.
12. Liu, Z.; Erhan, S.; Calvert, P. *J. Appl. Polym. Sci.* **2004**, *93*, 356.
13. Karger-Kocsis, J.; Grishchuk, S.; Sorochynska, L.; Rong, M. *Polym. Eng. Sci.* **2013**, *32*, 1879.
14. Wang, R.; Schuman, T. *Exp. Polym. Lett.* **2013**, *7*, 272.
15. Zhu, J.; Chandrashekhara, K.; Flanigan, V.; Kapila, S. *Compos. A.* **2004**, *35*, 95.
16. Parzuchowski, P. G.; Jurczyk-Kowalska, M.; Ryszkowska, J.; Rokicki, G. *J. Appl. Polym. Sci.* **2006**, *102*, 2904.
17. Thulasiraman, V.; Rakesh, S.; Sarojadevi, M. *Polym. Compos.* **2009**, *30*, 49.
18. Vary, A. In Non-Destructive Testing of Fibre-Reinforced Plastics Composites; Summerscales, J., Ed.; Elsevier: London, **1990**; Chapter 1.
19. Vary, A.; Bowles, K. *J. Polym. Eng. Sci.* **1979**, *19*, 373.
20. Srivastava, V.; Prakash, R. *Compos. Struct.* **1987**, *8*, 311.
21. Miyagawa, H.; Misra, M.; Drzal, L. T.; Mohanty, A. K. *Polym. Eng. Sci.* **2005**, *45*, 487.
22. Samper, M. D.; Fombuena, V.; Boronat, T.; García-Sanoguera, D.; Balart, R. *J. Am. Oil Chem. Soc.* **2012**, *89*, 1521.
23. Lakshmi, M. S.; Reddy, B. *Malaysian Polym. J.* **2010**, *5*, 84.
24. Singh, J.; Mishra, N. S.; Banerjee, S.; Sharma, Y. C. *BioResources.* **2011**, *6*, 2732.
25. Choi, S. S.; Nah, C.; Lee, S. G.; Joo, C. W. *Polym. Int.* **2003**, *52*, 23.
26. Tan, S. G.; Chow, W. S. *Exp. Polym. Lett.* **2011**, *5*, 480.
27. Czub, P. *Macromol. Symp.* **2006**, *245–246*, 533.
28. Jin, F.-L.; Park, S.-J. *Mater. Sci. Eng. A.* **2008**, *478*, 402.
29. Kumosa, L.; Benedikt, B.; Armentrout, D.; Kumosa, M. *Compos. A.* **2004**, *35*, 1049.
30. Park, S.-J.; Fan-Long, J.; Jae-Rock, L. *Mater. Sci. Eng. A.* **2004**, *374*, 109.
31. Crivello, J.; Narayan, R.; Sternstein, S. *J. Appl. Polym. Sci.* **1997**, *64*, 2073.
32. Park, S.-J.; Kim, T.-J.; Kim, H.-Y. *Polym. Int.* **2002**, *51*, 386.
33. Klason, C.; Kubat, J.; Strömvall, H.-E. *Int. J. Polym. Mater.* **1984**, *10*, 159.
34. Zaini, M.; Fuad, M. A.; Ismail, Z.; Mansor, M.; Mustafah, J. *Polym. Int.* **1996**, *40*, 51.
35. Matsumoto, A.; Kimura, T. *J. Appl. Polym. Sci.* **1998**, *68*, 1703.
36. López, J.; Gisbert, S.; Ferrándiz, S.; Vilaplana, J.; Jiménez, A. J. *Appl. Polym. Sci.* **1998**, *67*, 1769.